COBEM 2023 27TH INTERNATIONAL CONGRESS OF MECHANICAL ENGENEERING

ABCM Brazilian Society of Mechanical Sciences and Engineering
27th ABCM International Congress of Mechanical Engineering
December 04-08, 2023, Florianópolis-SC, Brazil

COB-2023-0987
NUMERICAL SIMULATION OF WATER HAMMER

José Gustavo Coelho
Federal University of Triângulo Mineiro - Av. Randolfo Borges Júnior, 1400 - Univerdecidade, Uberaba - MG, 38064-200
jose.gustavo@uftm.edu.br

André Luiz Amarante Mesquita
Laboratory of Fluid Dynamics and Particulate, FluidPar, Federal University of Pará, Av. Brasília, s/n, Vila Permanente, 68.455-901, Tucuruí, PA
andream@ufpa.br

Abstract. *Water hammer refers to pressure variations resulting from changes in flow caused by disturbances imposed on the flow of liquids in conduits, whether voluntary or involuntary. Examples of such disturbances include valve opening or closing operations, mechanical failures of protection and control devices, stoppage of hydraulic turbines, and pump shutdowns due to engine power failure. It is evident that this phenomenon can lead to significant losses across various industries, highlighting the importance of studying it to minimize costs and prevent accidents. In this research, the water hammer phenomenon is analyzed using Computational Fluid Dynamics (CFD) with ANSYS, a widely used commercial software. Both ANSYS-FLUENT and ANSYS-CFX are employed for analysis, utilizing numerical methodologies to investigate three-dimensional fluid flows. The study focuses on convergence analysis and explores the transient impacts of water hammer, examining the maximum pressure values and their temporal variations. Experimental data from the literature are used to validate the numerical results. Water is chosen as the fluid medium due to its compressible characteristics. Incompressible flow approximations yield inaccurate results for water hammer cases, necessitating the incorporation of compressibility characteristics for accurate numerical modeling. The research concludes with a detailed performance comparison of the two commercial software packages, assessing their accuracy under various conditions while considering computational costs. Both ANSYS-FLUENT and ANSYS-CFX demonstrate satisfactory results, with minimal errors compared to the experimental study. However, ANSYS-FLUENT exhibits greater computational efficiency, completing the simulations in less time.*

Keywords: *Computational Fluid Dynamics, ANSYS, Water Hammer*

1. INTRODUCTION

Hydraulic transients, commonly known as water hammer, manifest as a transient phenomenon resulting from the sudden deceleration of water within a confined system. This phenomenon gives rise to a notable surge in pressure immediately following the deceleration or acceleration of the fluid, subsequently propagating as a periodic pressure wave along the pipeline. As the wave oscillates back and forth within the conduit, it undergoes damping. The consequential water hammer effect can induce profound vibrations, posing significant hazards to both pipelines and essential equipment such as pumps and turbines. The acquisition of comprehensive data regarding pressure variation during this physical occurrence can be leveraged in the meticulous design of pipe networks. Consequently, precise estimation of the pressure surge during water hammer is of paramount importance in this context, warranting thorough investigation.

An application that necessitates a decelerating flow, akin to water hammer, pertains to the employment of the pressure-time method in hydropower flow measurement. This method capitalizes on the conversion of momentum into pressure during the deceleration of a liquid mass, resulting from the closure of a valve or guide vane, enabling the prediction of flow (International, 1991). The flow rate can be determined by integrating the differential pressure and accounting for pressure losses due to friction during water hammer, as expressed in Eq. (1).

$$Q = \frac{A}{\rho L}\int_0^{t_f}\left(\Delta p + \Delta p_f\right) dt + q, \tag{1}$$

where Q is the flow rate, L distance between measurement cross-sections, ρ the fluid density, t_f the final integration limit, A the cross-sectional area, Δp the differential pressure, Δp_f the pressure losses due to friction, and q the leakage flow rate

after valve closure. Accurate estimation of transient viscous losses during water hammer is imperative for precise flow rate calculations. However, the current evaluation method assumes one-dimensional flow, which significantly limits its applicability. Therefore, an extension of the evaluation method is necessary to accommodate variations in geometry and secondary flows. Consequently, three-dimensional numerical simulations are proposed as the next step to evaluate experimental data, thereby enhancing the overall accuracy of estimated flow rates.

Diverse boundary conditions were employed in prior investigations to simulate transient flow patterns. For example, (Anderson et al., 2001) utilized a combination of one-dimensional water hammer equations, solved using the method of characteristics (1D-MOC), and computational fluid dynamics (CFD) simulation to couple a pipe system with more intricate geometries, such as pumps or turbines. Additionally, 1D-MOC was employed to derive the variation of variables during the closure of a valve. These variables were applied to the interface between the one-dimensional and three-dimensional domains for transient CFD simulation of flow inside pumps and turbines. (Brumone and Berni, 2010) employed two-dimensional and three-dimensional CFD simulations to model water hammer during the closure of a gate valve. They demonstrated that a local recirculation zone emerged near the gate when the valve was closed in a downward direction, resulting in three-dimensional flow. However, a two-dimensional simulation could be substituted for a three-dimensional simulation when the distance from the gate exceeded 2.33D, as the recirculation zone created near the valve dissipated.

In the study of Brunone (Brunone et al., 2013) modified the outlet boundary condition to a wall boundary condition for modeling transient water hammer, simplifying the CFD simulation by eliminating the need to model the valve. Nevertheless, this approach is not entirely accurate, as the reduction in flow rate is not instantaneous. (Chaurdhry. 2014) implemented a velocity reduction at the outlet boundary instead of modeling the valve closure. They argued that this approach yielded improved agreement between CFD results and experimental data compared to the 1D-MOC. However, the flow rate reduction curve may not always be accessible, making the modeling of valve closure necessary for more faithful simulation results.

Various methods can be employed for modeling valve closure. The dynamic mesh method has been utilized to model the closure of axial gate valves (Brumone and Berni, 2010). In this method, the boundary moves and the mesh undergoes deformation. Das (1998) used total pressure at the inlet and static pressure at the outlet for the simulations. Remeshing using the dynamic mesh approach increases simulation time and can lead to divergence, particularly towards the end of valve closure when remeshing is performed in a smaller zone.

Guidaoui (Guidaoui, et al., 2005) adopted the sliding mesh method to model water hammer resulting from the closure of a spherical valve, which involves circular movement of the valve. The results indicated that the sliding mesh method is an accurate tool for modeling the rapid closure of ball valves with rotational movement. In this method, distinct zones move relative to each other. Despite the significant potential of this method, no study has yet utilized the sliding mesh method to model the closure of gate or sliding valves with vertical movement. Namgyun (Namgyun et al., 2013) conducts a study on water hammer using numerical simulation, employing ANSYS-CFX. Initially, a steady-state simulation is performed, followed by a change in the outlet boundary condition to a wall condition. The obtained results are compared to analytical and experimental data.

Mehrdad (Mehrdad et al., 2023), compares different methods for modeling water hammer. He utilizes the dynamic mesh, sliding mesh, and immersed solid methods, and compares the results with experimental data, which include the variation of pressure between two points and the wall shear stress. Additionally, he also compares the computational cost of these three numerical methods.

The present article introduces and investigates the prediction of 3D turbulent water hammer utilizing URANS equations while considering valve closure. The primary objectives of this study include investigating the water hammer phenomenon using simplified boundary conditions in the utilization of 3D URANS equations and conducting a comparative analysis of the results obtained from the CFX and FLUENT software packages, comparing them with experimental data.

2. METHODS

2.1 Experimental setup

The examined test instance of this research is founded on an experimental exploration carried out by Martins et al., 2016. The configuration represents a linear conduit with a consistent inner diameter of 0.02 m and 15.22 m of length. A diagram of the experimental setup employed for the investigation is depicted in Figure 1. The water is driven by gravitational force originating from a reservoir located at a vertical height H = 44.66 m relative to the measurement segment. The highest volumetric flow rate is $Q = 120.6 \times 10^{-3}$ l/s.

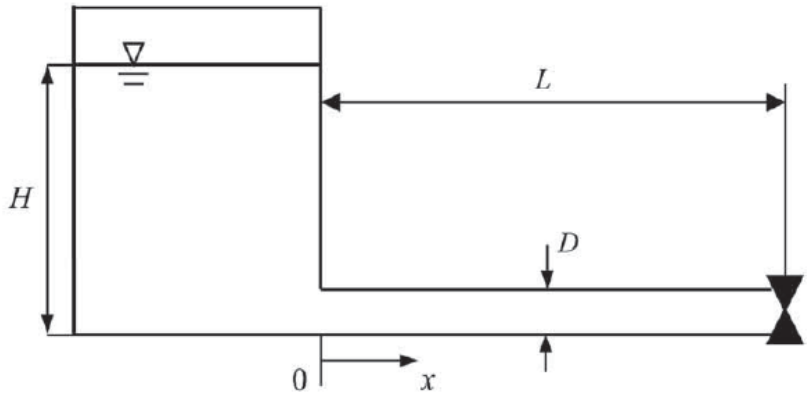

Figure 1: Schematic of the experimental set-up of Martins (Martins et al., 2016), where H = 44.66 m, L = 15.22 m, D = 0.02 m.

2.2 Mathematical modelling

The continuity and momentum equations for a time-dependent isothermal compressible turbulent flow are given by

$$\frac{\partial \rho}{\partial t} + \frac{\partial (\rho U_j)}{\partial x_j} = 0, \tag{2}$$

$$\frac{\partial (\rho U_i)}{\partial t} + \frac{\partial (\rho U_j U_i)}{\partial x_j} = -\frac{\partial P}{\partial x_i} + \frac{\partial}{\partial x_j}\left(\mu \frac{\partial U_i}{\partial x_j} - \rho \overline{u_\iota u_j}\right), \tag{3}$$

where P is the pressure, U_i the mean velocity, μ is the viscosity. To model the Reynolds shear stress term ($-\rho \overline{u_\iota u_j}$) in the turbulent flow, the k-ε model is used (Agarwal and Mthembu, 2020).

In ANSYS-FLUENT, we simply select the fluid as compressible. In ANSYS-CFX, some adjustments need to be made. For the simulation of compressible water, the following equation should be added to the governing equation:

$$\frac{d\rho}{\rho} = \frac{dP}{k_w}, \tag{4}$$

where k_w is the bulk modulus of water. Thus, the user has the capability to designate the density by employing the equation that establishes the connection between density and pressure, integrating Eq. (4), we obtain Eq. (5).

$$\int_{\rho_0}^{\rho_w} \frac{d\rho}{\rho} = \int_{P_{atm}}^{P} \frac{dP}{k_w} \rightarrow \ln \rho_w - \ln \rho_0 = \frac{P - P_{atm}}{k_w} \rightarrow \rho_w = \rho_0 \cdot exp\left(\frac{P - P_{atm}}{k_w}\right), \tag{5}$$

where ρ_0 is the initial density, ρ_w is the water density, P_{atm} the atmospheric pressure. In this study, ρ_0 is et to 997 kg/m^3 and the bulk modulus of water, k_w, is assumed as a constant value, 2.15x10^9 Pa.

2.3 Numerical modelling

To conduct the simulation, a straightforward cylindrical conduit is employed. The pipe has a diameter of 0.02 meters and a length of 15.22 meters. The geometric configuration and boundary conditions are illustrated in Figure 2. The simulation is performed in two stages. Initially, the steady flow within the pipe is computed by applying the pressure boundary condition at the inlet and velocity boundary condition at the outlet, with a convergence criterion set to 10^{-5} using RMS (Root Mean Square). At the inlet, the pressure equivalent to a height of 44.66 m is applied. The fluid motion is induced by the pressure disparity between the inlet and outlet, ultimately reaching a stable state. Subsequently, a transient simulation is performed to study the water-hammer phenomenon. The outlet boundary is transitioned to operate at a

specified velocity, as defined by Eq (6). As a pressure wave emerges, the velocity direction at the inlet undergoes periodic changes. The time step used for the transient simulation is 4 seconds.

$$if(t \leq a) \quad (6)$$
$$veloc = b$$
$$else$$
$$veloc = c$$

where t is the simulation time, a is the valve closing time, and b is the flow velocity. When the simulation time exceeds t, it assumes a velocity of zero, simulating the effect of valve closure. In this study, a = 0.28 s, b = 0.384 m/s and c = 0 m/s.

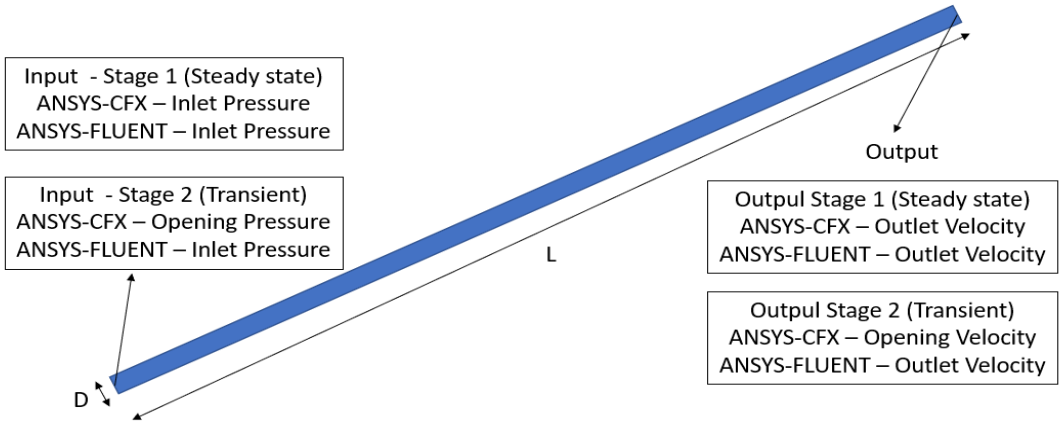

Figure 2: Geometry, where D = 0.02 m, L = 15.22 m and the boundary condition used in the simulation.

The mesh study was conducted to ensure that the mesh does not influence the results. We employed a mesh with 411910 nodes (363375 elements) and another with 12575888 nodes (12117234 elements). We compared the results for the first pressure wave. The greatest discrepancy occurs during the rapid pressure variation, with a difference on the order of 5%. However, after this moment, the results become comparable. Therefore, the mesh with lower computational cost was chosen, as it yielded satisfactory data throughout the simulation. A comparison between these results is depicted in Figure 3.

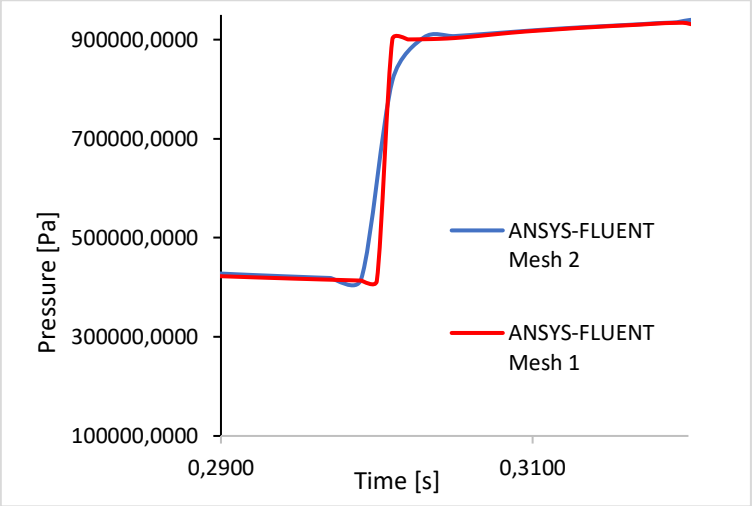

Figure 3: Mesh Comparison. Mesh 1 consists of 12575888 nodes, whereas Mesh 2 contains 411910 nodes.

ANSYS-CFX and ANSYS-FLUENT software packages employ different methods for solving the governing equations, rendering a simple comparison unreasonable. Therefore, two configurations of Fluent and one of CFX were utilized, and a comparison of the results and the times obtained was conducted. The ANSYS-CFX uses the coupled finite volume method for resolving the equations. The high-resolutions scheme is used for the advection scheme, and the timestep is 0.0014 s for the transient simulation. The ANSYS-FLUENT software offers bi-dimensional and tri-dimensional simulation options. We have chosen to focus solely on tri-dimensional situations for analysis purposes. In the first Fluent configuration, the SIMPLE algorithm is employed to ascertain the pressure field, while the nonlinear convective terms in all transport equations are approximated using Second Order for Pressure and First Order Upwind for other equations. In another Fluent configuration, the PISO (Pressure-Implicit with Splitting of Operators) algorithm is utilized to determine the pressure field. In both situations, the timestep employed for the transient simulation is 0.0014 s.

3. RESULTS

Figure 4 presents the comparison between the computed pressure distribution and the measured data by Martins et al., (2016) at the final section (at 15.22 m). Slightly before valve closure (prior to 0.29 s), ANSYS-FLUENT (SIMPLE) exhibited a slight oscillation, in contrast to ANSYS-CFX and the experimental data. The first pressure peak occurs instantaneously, with the pressure rising from 444 kPa to 920 kPa within a 0.005 s interval, and both commercial software packages achieved satisfactory results in capturing this abrupt pressure variation. Both the maximum peak and the onset of pressure decrease closely approximated the experimental measurements. The pressure decreases also transpired abruptly, dropping from 894 kPa to -19kPa within 0.0075 s. Once again, both software packages obtained satisfactory results in capturing this phenomenon. Furthermore, between the time interval of 0.29 s and 0.47 s, the phenomenon exhibited 4 peaks and 3 troughs. Both ANSYS-CFX and ANSYS-FLUENT (SIMPLE) yielded good results during all these periods.

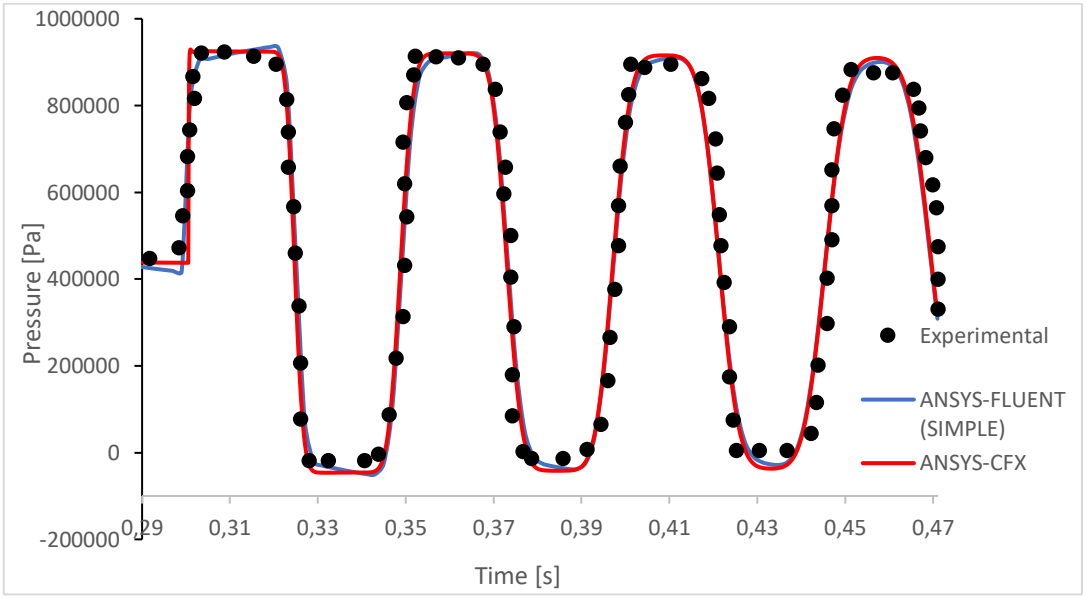

Figure 4: Analysis of numerical results obtained with ANSYS-CFX, ANSYS-FLUENT (SIMPLE), in comparison with experimental data found in Martins et al., (2016).

Table 1 depicts the computed average pressure distribution at the end of the pipeline using ANSYS-CFX. At time 0.25 s, the pressure is 437.755 kPa, which is measured before valve closure. Subsequently, upon valve closure, the pressure rapidly increases, reaching its peak when the pressure reaches 924.608 kPa. This value remains constant from 0.3009 s to 0.321 s before the pressure begins to decrease. The next measurement is 849.176 kPa at a time of 0.3225 s. As previously mentioned, the pressure variation is extremely rapid. After this, the pressure reaches negative values, with a pressure of -46.171 kPa at a time of 0.3295 s, remaining at this level until 0.3431 s. Subsequently, the pressure starts to rise again. At time 0.3485 s, the pressure is 377.342 kPa. The pressure surpasses the initial value once more, reaching

699.877 kPa at a time of 0.3505 s, entering another peak region indicated with a pressure of 920.107 kPa at a time of 0.3561 s. It remains at this level until 0.3657 s, after which it starts to decrease again. At 0.3710 s, the pressure of 790.642 kPa is reached. It is evident that within a time interval of 0.07 s, the water hammer phenomenon caused a significant pressure variation, which was accurately captured by the numerical software.

Figure 5 shows the velocity profile calculated at a distance of 10 m from the inlet region. In a), measured at 0.27 s, we have the measurement taken before the valve closure. As we can see, the velocity profile represents fully developed flow. In b), measured at 0.29 s, there is a decrease in velocity, but it still exhibits characteristics of developed flow behavior. In c), measured at 0.32 s, it is noticeable that the flow is recirculating due to the valve closure. As expected, a certain amount of time is required for the flow to propagate from the outlet region, where the valve closure takes place, to the measured point. Meanwhile, at point d), calculated at 0.34 seconds, the flow begins to return to its original state.

Table 1: Average pressure distribution at the end of the pipeline at different time instants.

Time [s]	Pressure [kPa]
0.2500 s	437.755
0.3009 s	924.608
0.3225 s	849.176
0.3295 s	-46.171
0.3485 s	377.342
0.3505 s	699.877
0.3561 s	920.107
0.3701 s	790.642

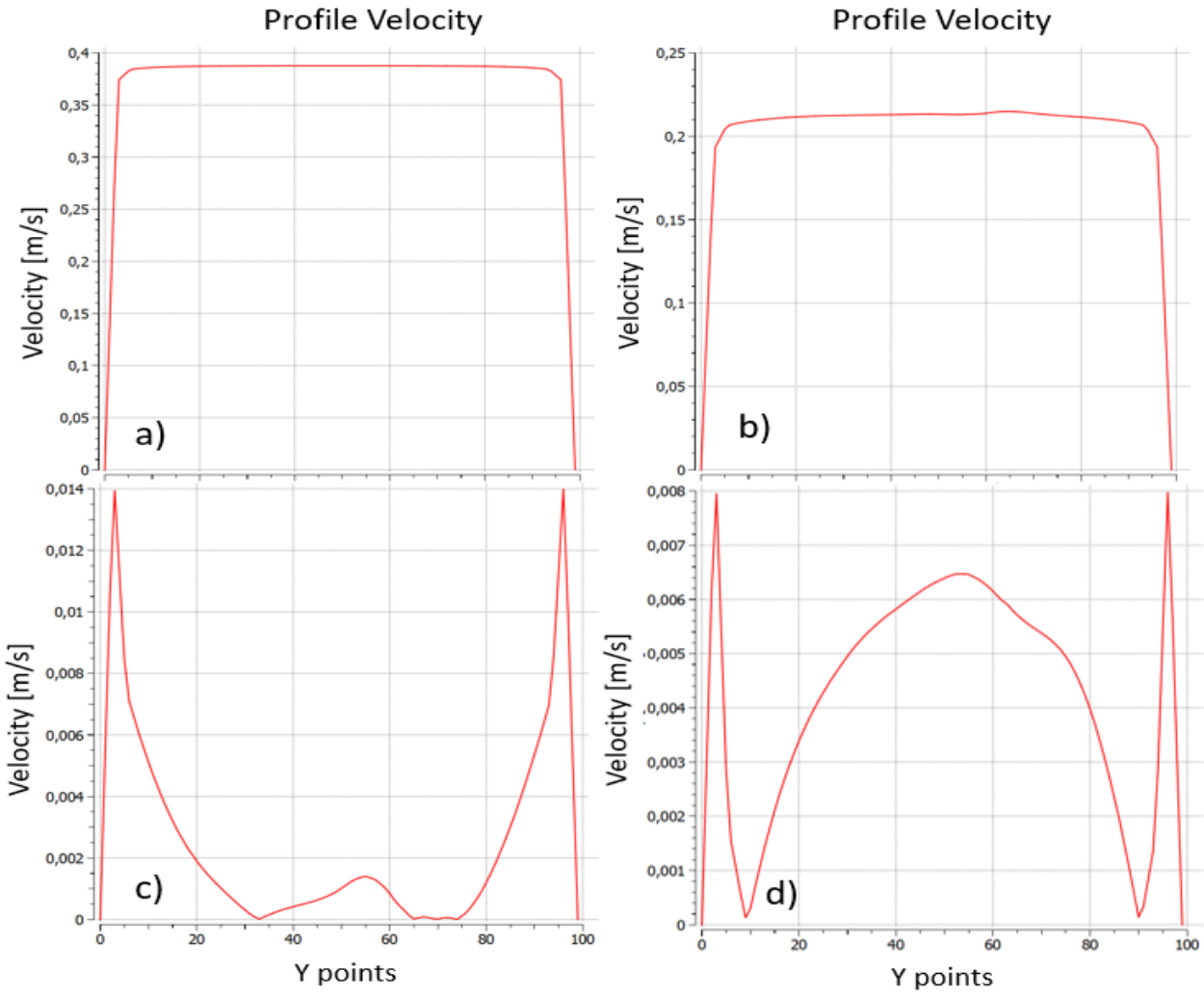

Figure 5: Velocity profile at different times, where a) 0.25 s, b) 0.31 s, c) 0.33 s and d) 0.34 s.

The simulations were conducted on the same computer, and the fundamental configurations are outlined in Table 2. Furthermore, the computational time expended by each software is provided. The total simulation time for ANSYS-CFX was 3.10 hours. As previously mentioned, two configurations were employed for Fluent. One utilized a simplified equation resolution approach employing SIMPLE, while the other employed a more intricate pressure-velocity coupling scheme known as PISO. With SIMPLE, the simulation time amounted to 1.19 hours, whereas with PISO, it was 16.7 hours. As can be observed, the utilization of this ANSYS-FLUENT (PISO) configuration significantly increased the simulation time without presenting apparent advantages for the analyzed case.

Table 2: Computational resources and lime allocated to the simulations.

Software	Number of CPU (GHz)	Memory (GB)	App. Time (h)
ANSYS-CFX	6 (2.4 GHz)	128 GB	3.10 h
ANSYS-FLUENT (SIMPLE)	6 (2.4 GHz)	128 GB	1.19 h
ANSYS-FLUENT (PISO)	6 (2.4 GHz)	128 GB	16.7 h

4. CONCLUSIONS

In this study, a numerical simulation of water hammer, a phenomenon characterized by a rapid pressure variation within a short time interval, was conducted. To accurately model the flow, it is crucial to consider compressible characteristics, even when dealing with water as the fluid. Two widely used commercial software packages, ANSYS-FLUENT and ANSYS-CFX, were employed for the numerical analysis to compare the obtained results. Experimental data from Martins et al. (2016) were used as a reference to validate the results. The simulation outcomes demonstrated that both software packages yielded satisfactory results. They successfully captured the rapid pressure variation and the periodic behavior of pressure in the vicinity of the closing valve.

In addition to the quantitative results, we also conducted an analysis of the computational performance of each software. Given that these software packages employ distinct methods for solving the governing equations, we employed one configuration for ANSYS-CFX and two for ANSYS-FLUENT. The quickest solution was obtained with ANSYS-FLUENT (SIMPLE). In contrast, when using the ANSYS-FLUENT (PISO) configuration, the simulation ran slower than with ANSYS-FLUENT (SIMPLE). Thus, for the analyzed case, both software packages demonstrated their reliability in addressing the proposed problem, with the simplified ANSYS-FLUENT configuration proving to be the swiftest solution.

5. ACKNOWLEDGEMENTS

The authors would like to thank the Conselho Nacional de Desenvolvimento Científico e Tecnológico (CNPQ) for supporting this research through the CNPq/MCTI/FNDCT Nº 25/2022 “Methodologies for Evaluation and Sizing of Low and Ultra Low Head Axial Turbines”.

6. REFERENCES

Agarwal A. and Mthembu L. *CFD analysis of conical diffuser under swirl flow inlet conditions using turbulence models*. Materials Today: Proceedings 27 (2020) 1350 –1355.

Anderson W. K., Newman J. C., Whitfield D. L., Nielsen E. J. Sensitivity analysis for Navier–Stokes equations on unstructured meshes using complex variables. AIAA J 2001; 39 (1):56–63.

Brunone B. and Berni A. Wall shear stress in transient turbulent pipe flow by local velocity measurement. Journal Hydraulic Engineering 2010; 136 (10): 716– 26.

Brunone B., Ferrante M., Meniconi S., Massari C. Effectiveness assessment of pipe systems by means of transient test-based techniques. Procedia Environment Science 2013; 19: 814–22.

Chaudhry M. H. Applied Hydraulic Transients, Textbook, 2014, Springer, 583 p.

Das D., Arakeri J. H. Transition of unsteady velocity profiles with reverse flow. Journal Fluid Mechanics 1998; 374: 251–83.

Ghidaoui M. S., Zhao M., McInnis D. A., Axworthy D. H. A review of water hammer theory and practice. Applied Mechanic Review 2005 (49): 58 – 76.

International Electrotechnical Commission 60041. Field Acceptance Tests to Determine the Hydraulic Performance of Hydraulic Turbines, Storage Pumps and Pump-Turbines. International Electrotechnical Commission: Geneva, Switzerland, 1991.

Mehrdad K. N., Georgiana D., Pontus J. Michel J. C. A Comparison of Different Methods for Modelling Water Hammer Valve Closure with CFD, Water 2023, 15, 1510.

Martins M. C. N., Alexandre K. S., Helena M. R., Dídia I. C. C. CFD modeling of transient flow in pressurized pipes. Computers and Fluids 126 (2016) 129–140.

Namgyun J., Daeyoung C., Juhyeon Y. Analytic estimation of the impact pressure in a beam-tube due to water-hammer effect. Journal of Nuclear Science and Technology, 2013, Vol. 50, No. 12, 1139–1149.

7. RESPONSIBILITY NOTICE

The authors are the only responsible for the printed material included in this paper.